A&A 669, A103 (2023)
https://doi.org/10.1051/0004-6361/202244832

Astronomy & Astrophysics

A giant umbrella-like stellar stream around the tidal ring galaxy NGC 922

David Martínez-Delgado[1], Santi Roca-Fàbrega[2,3,4], Juan Miró-Carretero[3], Maria Angeles Gómez-Flechoso[3,4], Javier Romàn[5,6,7], Giuseppe Donatiello[8], Judy Schmidt[9], Dustin Lang[10], Mohammad Akhlaghi[11], and Mark Hanson[12]

[1] Instituto de Astrofísica de Andalucía, CSIC, Glorieta de la Astronomía, 18080 Granada, Spain
e-mail: dmartinez@iaa.es
[2] Instituto de Astronomía, Universidad Nacional Autónoma de México, Apartado Postal 106, 22800 Ensenada, BC, Mexico
[3] Departamento de Física de la Tierra y Astrofísica, Universidad Complutense de Madrid, 28040 Madrid, Spain
[4] Instituto de Física de Partículas y del Cosmos (IPARCOS), Fac. CC. Físicas, Universidad Complutense de Madrid, Plaza de las Ciencias, 1, 28040 Madrid, Spain
[5] Kapteyn Astronomical Institute, University of Groningen, PO Box 800, 9700 AV Groningen, The Netherlands
[6] Instituto de Astrofísica de Canarias, c/ Vía Láctea s/n, 38205 La Laguna, Tenerife, Spain
[7] Departamento de Astrofísica, Universidad de La Laguna, 38200 La Laguna, Spain
[8] UAI – Unione Astrofili Italiani /P.I. Sezione Nazionale di Ricerca Profondo Cielo, 72024 Oria, Italy
[9] Astrophysics Source Code Library, University of Maryland, 4254 Stadium Drive, College Park, MD 20742, USA
[10] Perimeter Institute for Theoretical Physics, 31 Caroline St N, Waterloo, Canada
[11] Centro de Estudios de Física del Cosmos de Aragón (CEFCA), Unidad Asociada al CSIC, Plaza San Juan 1, 44001 Teruel, Spain
[12] Stan Watson Observatory South, Dark Sky New Mexico, Animas NM 88020, USA

Received 29 August 2022 / Accepted 7 October 2022

ABSTRACT

Context. Tidal ring galaxies (TRGs) are rarely observed in the local universe due to their intrinsically transient nature. The tidal ring structures are the result of strong interactions between gas-rich stellar disks and smaller galactic systems, and do not last longer than ~500 Myr. Therefore, these are perfect scenarios in which to look for the debris of recently accreted dwarf galactic systems.
Aims. Our goal is to study the low surface brightness stellar structures around the TRG NGC 922 and to revise the hypothesis of its formation in light of these new data.
Methods. We present new deep images of the TRG NGC 922 and its surroundings from the DESI Legacy survey data and from our observations with an amateur telescope. These observations are compared with results from high-resolution N-body simulations that were designed to reproduce an alternative formation scenario for this peculiar galaxy.
Results. Our new observations unveil that the low surface brightness stellar tidal structures around NGC 922 are much more complex than reported in previous works. In particular, the formerly detected tidal spike-like structure at the north-east of the central galaxy disk is not connected with the dwarf companion galaxy PGC 3080368, which has been suggested as the intruder triggering the ring formation of NGC 922. The deep images reveal that this tidal structure mainly has a fainter giant umbrella-like shape, and thus it was formed from the tidal disruption of a different satellite. Using the broad-band g, r, and z DESI LS images, we measured the photometric properties of this stellar stream, estimating a total absolute magnitude in the r band of $M_r = -17.0 \pm 0.03$ mag and a total stellar mass for the stream of between 6.9 and 8.5×10^8 $M_\odot$. We performed a set of N-body simulations to reproduce the observed NGC922-intruder interaction, suggesting a new scenario for the formation of its tidal ring from the infall of a gas-rich satellite around 150 Myr ago. Finally, our deep images also reveal a tidal shell around the dwarf galaxy PGC 3080368, a possible fossil of a recent merger with a smaller satellite, which may suggest it is in its first infall towards NGC 922.

Key words. galaxies: interactions – galaxies: structure – galaxies: clusters: individual: NGC 922

1. Introduction

The widely accepted theory for galaxy formation and evolution proposes that galaxies grow through two main channels: gas accretion through filaments, and mergers with other galactic systems (e.g., L'Huillier et al. 2012). These processes lead to the formation of a zoo of galaxy morphologies that was described by the classical Hubble sequence (Willett et al. 2013). Furthermore, observations show that a non-negligible fraction of the local universe galaxies have peculiar morphologies not initially included in this classification (Nair & Abraham 2010; Willett et al. 2013). Among them, ring galaxies are particularly abundant (Willett et al. 2013) as they are present in more than one fifth of spiral galaxies (Buta & Combes 1996). Their origin has been studied from the early development of numerical astronomy using N-body simulations (e.g., Lynds & Toomre 1976; Gerber et al. 1992; Hernquist & Weil 1993). Also, experts on galactic dynamics used analytical approaches to unveil the origin of such structures (Struck-Marcell 1990; Kormendy & Kennicutt 2004; Romero-Gómez et al. 2007). In light of results from these many works, researchers agree that ring-like galactic systems can form through two mechanisms (Buta & Combes 1996): a secular process triggered by the presence of a galactic bar (Romero-Gómez et al. 2007), and strong interactions with other galactic systems (Wu & Jiang 2012). Although both

mechanisms produce similar morphologies, the properties of the resulting rings are well differentiated. Rings of secular origin are Θ-shaped (O-type), do not show expansion velocity, and are not or marginally star forming. Rings resulting from interactions (P-type) show strong star formation within the ring and the central region of the galaxy, in most cases show a clear expansion velocity outwards, and present a variety of shapes.

Although collisions during minor mergers are common in the cold dark matter (CDM) paradigm, most collisional rings in the low-z universe are of secular origin. In fact, the statistics of observed and simulated ring galaxies show that the presence of ring-like galaxies by collisions (Tidal Ring Galaxies, TRG hereafter) is especially relevant at high redshifts, when mergers dominate the galaxy growth (Elagali et al. 2018a), while the secular processes are prevalent at lower-z and in low-density environments, where galaxies tend to be less perturbed. This agrees well with the most recent observations of collisional rings in galaxies of the local universe (e.g., CSRG and CZ2-CNRG, Buta 1995, 2017) that, according to Madore et al. (2009), show a lower limit of only 0.001%. In Madore et al. (2009), the authors also state that, if assuming a constant minor mergers rate, it is expected that in the local volume, the majority of galaxies should have suffered a collisional ring formation over a Hubble time (see also Theys & Spiegel 1976). Therefore, the low number of detections is due to the short dynamical time of its formation, evolution, and decay.

After several years of research, many studies showed that the TRGs are produced by an impulsive interaction between a small galaxy (intruder) in an almost radial orbit and the gaseous disk of a larger galaxy (e.g., Madore et al. 2009). The short but strong interaction of the intruder with the disk of the larger galaxy make it contract first and then later expand, resulting in an outwardly propagating wave (Lynds & Toomre 1976; Hernquist & Weil 1993). This compression wave triggers star formation in an expanding ring that can reach velocities up to $\sim$113 km s^{-1} just after the collision ($\sim$50 Myr, e.g., Arp 147, Fogarty et al. 2011), slowing down to $\sim$50 km s^{-1} for older rings ($\sim$200 Myr, e.g., Cartwheel galaxy, Higdon 1996). Properties of the ring and the survival of the bar and/or bulge in the centre of the disk are determined by the mass of the intruder and its impact parameter with respect to the centre of the disk (Gerber et al. 1996; Madore et al. 2009; Fiacconi et al. 2012; Elagali et al. 2018b). All models and simulations showed that these star-forming rings only last for 0.2−0.5 Gyr (Wong et al. 2006; Pellerin et al. 2010; Renaud et al. 2018; Elagali et al. 2018a) and they became only marginally observable up to 0.7 Gyr after the collision (Wu & Jiang 2015), which makes them transient features. The identification of the intruder can also be challenging. Interacting dwarf galaxies can be quickly disrupted and mixed with the central regions of the TRG (Madore et al. 2009), either in their first or second pericentre (Wu & Jiang 2015). In this regard Elmegreen & Elmegreen (2006) showed that some observed TRGs have no obvious companions and that this can be due to the fact that observations are not deep enough or because the companions have already merged with the main galaxy. Some works also pointed out the possibility that multiple perturbers, or multiple interactions by a single intruder, can generate prominent rings.

From an observational point of view, the most prominent example of a TRG is the Cartwheel galaxy. This system has been studied and simulated by many research groups (e.g., Charmandaris et al. 1999; Mayya et al. 2005; Barway et al. 2020), which helped to clarify the picture of the formation and evolution of such systems. Another example of a Cartwheel-like system is the less studied NGC 922. Wong et al. (2006) proposed that the nearby compact dwarf PGC 3080368 (named S2 in their work) could be the intruder that generated the observed TRG morphology on NGC 922. In their work, the authors presented an N-body simulation showing that an off-centre impact of a point mass on NGC 922-like disk galaxy can generate a TRG. However, their models cannot fully explain the formation and morphology of the detected stellar plume around NGC 922 (Pellerin et al. 2010). More recently, HI observations of NGC 922 and its outskirts have found an HI tail that is neither aligned with the S2 orbit nor with the stellar plume (Elagali et al. 2018b). This result suggests than an interaction other than the one proposed by Wong et al. (2006) occurred with NGC 922. In Elagali et al. (2018b), the authors did not find the HI bridge predicted by all hydrodynamical models of similar interacting systems that should connect S2 to NGC 922. In addition, although showing a Cartwheel-like morphology in observations in the optical, this system does not show the single drop-out TRG typical morphology in HI or in the stellar component as predicted by simulations (Elagali et al. 2018a; Renaud et al. 2018). All these inconsistencies found when comparing data with results from numerical experiments points towards a more complex formation scenario than the one proposed by Wong et al. (2006).

In this paper, we present new deep images of the TRG NGC 922 and its surroundings from the DESI Legacy survey data and from our observations with an amateur telescope. These observations are compared with results from high-resolution N-body simulations that were designed to reproduce an alternative formation scenario for this peculiar galaxy. This paper is organized as follows. In Sect. 2 we describe the observations that we use in this work to support our new hypothesis on the formation of the TRG NGC 922. In Sect. 3 we present our main results obtained after analysing the observations. The N-body models used in this work are described in Sect. 4. Finally, in Sects. 5 and 6, we discuss our results and present our conclusions.

2. Observations and data reduction

2.1. Stan Watson Observatory South RC-60 cm telescope

A wide-field deep image of NGC 922 and its tidal stream was obtained at the Stan Watson Observatory South (Dark Sky New Mexico, USA) with a 60 cm aperture $f/6.7$ Planewave CDK Ritchey-Chrétien telescope. We used an SBIG STX16803 CCD camera that provided a pixel scale of 0.46″ pixels^{-1} over a 32.0′×32.0′ field of view. We obtained a set of 40 individual 900-second images with an Astrodon Gen2 Tru-Balance E-series luminance filter[1] over several nights between 2021 November, 25 and 2021 November, 29 through remote observations. Each individual exposure was reduced following standard image processing procedures for dark subtraction, bias correction, and flat fielding (Martínez-Delgado et al. 2010). The images were combined to create a final co-added luminance-filter image with a total exposure time of 36 000 s (see Fig. 1, top panel).

2.2. DESI Legacy surveys imaging data

NGC 922 is one of the target galaxies of the Stellar Stream Legacy Survey (Martinez-Delgado et al. 2021), which is carrying out a systematic search for stellar tidal streams around massive galaxies in the local universe. The imaging sources for this project are: (1) the DESI Legacy Imaging Surveys (DESI LS), which compile optical data in three optical bands (g, r,

[1] This filter transmits from 400 $\lesssim \lambda$ (nm) $\lesssim$ 700, and broadly covers the g and r bands.

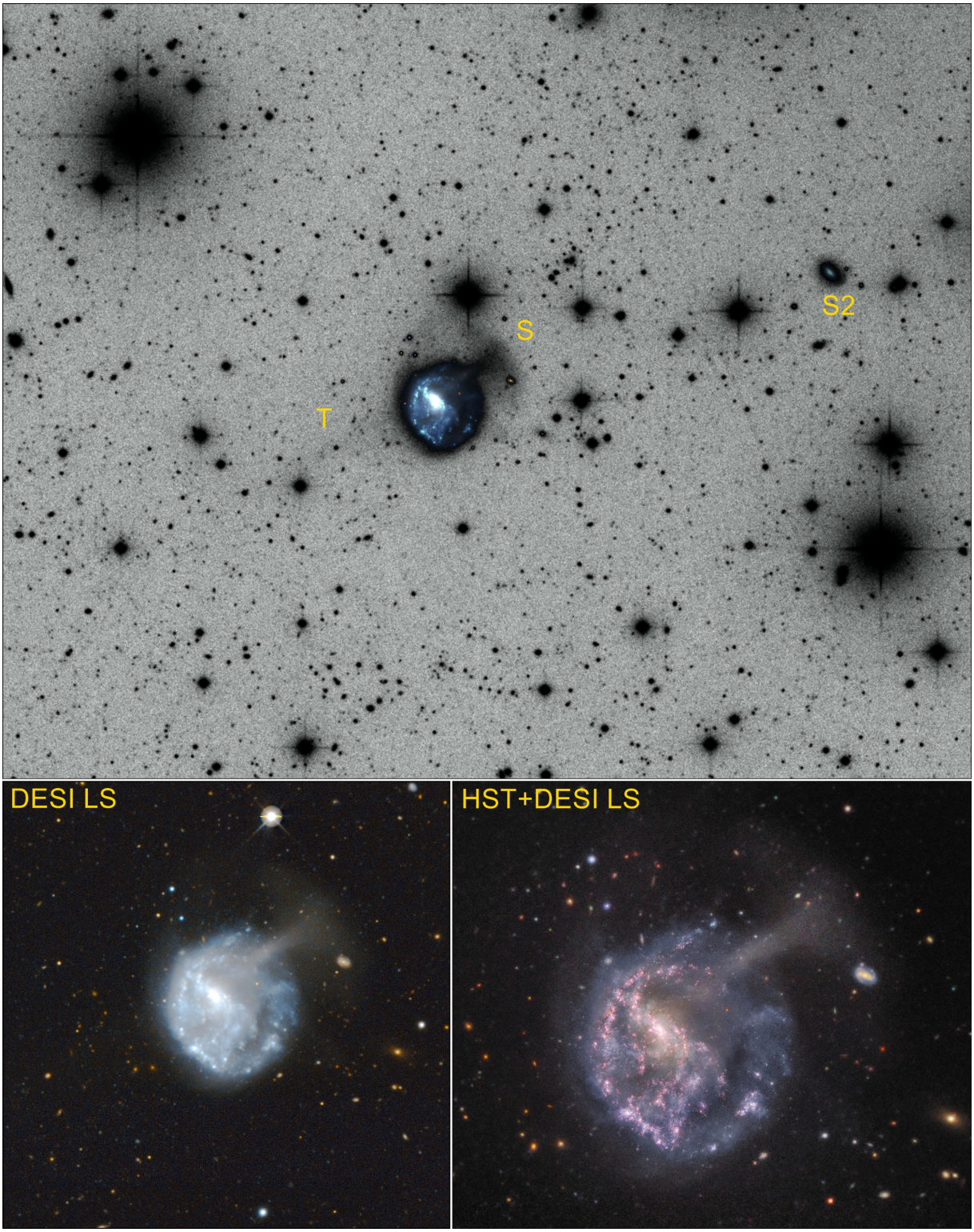

Fig. 1. Deep images of the NGC 922 stellar tidal stream. *Top*: RC-60 cm telescope luminance-filter image including NGC 922, its stellar tidal stream (whose two components are marked with labels T and S), and the PG3080368 dwarf galaxy (marked with the label S2). *Bottom left*: DESI LS colour image cutout of NGC 922 and its stream obtained with legacypipe, as described in Sect. 2.2. *Bottom right*: zoomed, higher-resolution view of the star formation regions of the NGC 922 disk and the stellar stream from a composition of public available *Hubble* Space Telescope images and the DESI Legacy survey data used in this work.

and z) obtained by three different imaging projects: the DECam Legacy Survey (DECaLS), the Beijing-Arizona Sky Survey (BASS) together with the Mayall z-band Legacy Survey (MzLS) (Zou et al. 2019; Dey et al. 2019), and the re-reduced public DECam data from the Dark Energy Survey (DES; Abbott et al. 2018).

In the bottom left panel of Fig. 1, we show an image cutout centred on NGC 922 obtained by co-adding images of this

galaxy taken by the DES (Abbott et al. 2018) using the DECam. These data were reprocessed using the LEGACYPIPE software of the DESI LS (see e.g., Fig. 2 in Martinez-Delgado et al. 2021). In short, each image of this survey, including NGC 922, was astrometrically calibrated to *Gaia*-DR2 and photometrically calibrated to the Pan-STARRS PS1 survey. Then they were subsequently resampled to a common pixel grid and summed with inverse-variance weighting.

The depth of the DESI LS images in each band was determined by calculating the surface brightness limit following the standard method of Román et al. (2020), that is, the surface brightness corresponding to 3σ of the signal in the non-detection areas of the image for a 100 arcsec^2 aperture (Martinez-Delgado et al. 2021). This yielded 29.15, 28.73, and 27.52 mag arcsec^{-2} for the g, the r and the z passbands, respectively.

2.3. Photometry of the NGC 922 stream

The photometry of the stellar stream around NGC 922 in the g, r, and z bands were derived with the GNU Astronomy Utilities (Gnuastro)[2] using the resulting co-added image cutout of this galaxy from the DESI LS data (see Sect. 2.2). The measurements were carried out with Gnuastro's MAKECATALOG on the basis of the sky-subtracted image generated by Gnuastro's NOISECHISEL (Akhlaghi & Ichikawa 2015; Akhlaghi 2019).

In addition to the photometry of NGC 922 stream obtained from this custom Legacy Surveys cutout image, we also fitted a Sérsic model to the disk of NGC 922 in order to subtract spurious flux where the stream is located. Although this modelling does not contain structural information of NGC 922 given its irregular morphology, it is useful to reduce systematic errors and provide the cleanest possible photometry in external regions of the disk, where the stream stands out and is susceptible to analysis. The most important procedure here is to obtain a correct masking. In this regard we masked all external sources, and thus we exclusively fitted the disk contribution. Once the mask was defined, the fitting was performed to the unmasked flux by χ^2 minimization of using `IMFIT` (Erwin 2015). We tested with different masks, more or less aggressive, coming to the conclusion that the fitted model is robust within the inevitable residuals in the inner regions due to the irregular morphology of the galaxy. However, in the outermost parts where the tidal features are found, the residuals are fairly clean. For simplicity, and to not add unnecessary parameters that could cause more residuals in the outer regions, the model we fitted was a simple Sersic function that had a single variable (n). Since the galaxy model used for the subtraction was not fully optimized for this type of irregular spiral galaxy, we only used it in our photometric analysis to quantify the possible contamination of the outer disk of the host galaxy on the surface brightness, colour, and luminosity measurements of the stream, as it is discussed in Sec. 3.2.

3. Results

3.1. The umbrella-like stellar stream of NGC 922

The deep images of NGC 922 detected tidal structures in its outskirts at a much lower surface brightness than previous studies and, thus, allowed us to interpret their origin in more detail than in previous works. Figure 1 shows that the halo of NGC 922 contains a giant, complex low surface brightness umbrella-like

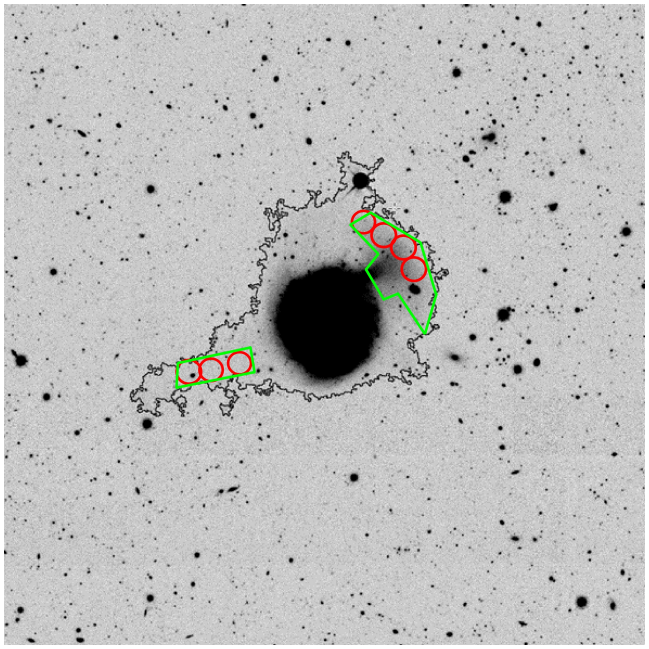

Fig. 2. Photometry measurement method for the stellar stream around NGC 922. The apertures where the photometry parameters, surface brightness, and colours are measured both for the 'shell' and the 'tail' parts of the stream are highlighted in red. The polygonal apertures (green) indicate the parts of the image used to measure the magnitude of the stream. The contour of the detection, encompassing the galaxy and the stream, is highlighted by a black line. Here the input image has been warped to a pixel grid 8×8 coarser than the original one, to highlight the low surface brightness signal.

substructure connected to the aforementioned bright, collimated tidal plume detected in many previous studies (see Sect. 1) and is also visible in the *Hubble* Space Telescope (HST) data of this galaxy (Fig. 1, bottom right panel). Interestingly, both amateur (Fig. 1, top panel) and DESI LS (Fig. 2) images also reveal a very faint, tail-like feature on the south-east side of NGC 922 (marked with T in Fig. 1 top panel), which seems to be the extension of the plume on the other side of the disk, following the path of the radial orbit of the disrupted satellite (see Sect. 4). Thus, our observations suggest that all these tidal structures were formed by a different satellite than the nearby compact dwarf (named S2) proposed by Wong et al. (2006), which appears clearly isolated and with no signature of a tidal tail emanating in the direction of NGC 922. Because of their shallower data, they assumed that the brighter tidal plume, roughly in the direction of the S2 dwarf, was the only signature of a recent strong interaction of those galactic systems.

The overall tidal structure observed around NGC 922 is quite similar to that of the well-known umbrella-like galactic systems (e.g., NGC 4651, Foster et al. 2014), which are the consequence of the recent tidal disruption of a satellite galaxy orbiting in a radial orbit in the main galaxy outskirts. Our simulations agree with these previous works (see Sect. 4). Therefore, we state that there is no causal connection between S2 and the formation of this low surface brightness structure.

Our deep amateur image also includes the S2 dwarf galaxy, which is clearly visible on the upper right side of our amateur image (marked with S2 in Fig. 1, top panel). This kind of system is expected to suffer a strong star formation burst after interacting with a central galaxy, followed by a fast depletion of gas, as a consequence of the gas consumption in star formation and

[2] http://www.gnu.org/software/gnuastro

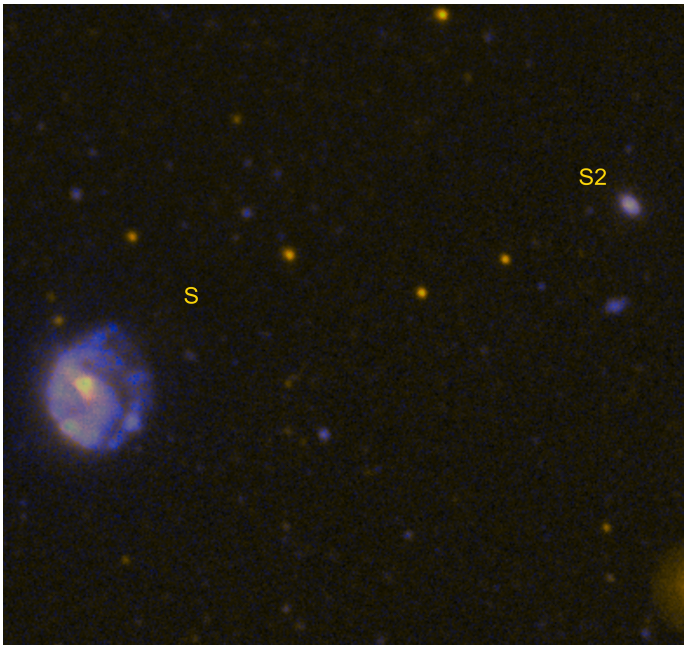

Fig. 3. Image of NGC 922 (labelled with S) and its companion S2 (*top right*) from the GALEX GR6/7 data release. This GALEX-UV image shows that both systems host strong UV emission, which may indicate active star formation. As it is mentioned in Fig. 4, the UV-luminous smaller galaxy to the south of S2 is possibly a background distant galaxy. The field of view is about 10.5×10.5 arcmin. North is up and east is left.

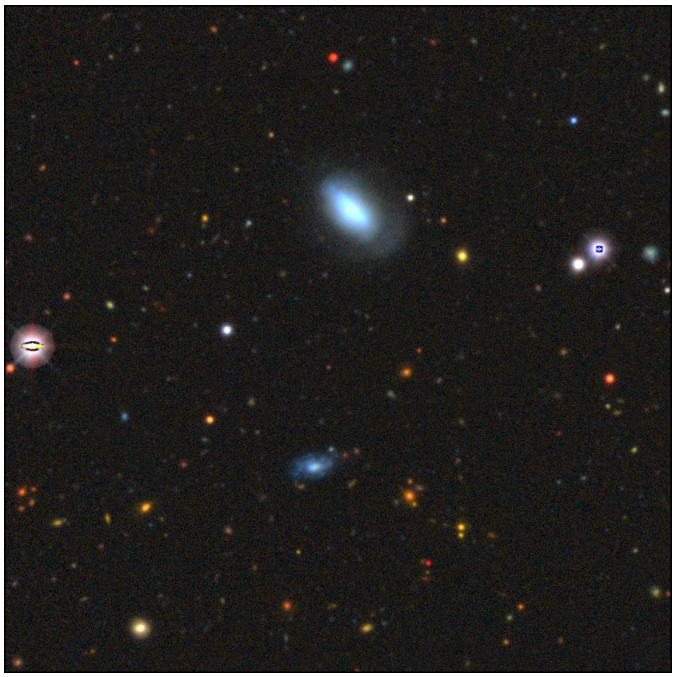

Fig. 4. DESI Legacy image cutout of the compact dwarf galaxy PGC 3080368, the S2 intruder galaxy in Wong et al. (2006). This deep image reveals an outer shell on its south-west side, also detected in the amateur data shown in Fig. 1 (*top panel*). The blue smaller galaxy to the south of S2 is possibly a background distant galaxy. The field of view is about 4×4 arcmin. North is up and east is left.

the clearance by supernovae feedback. Less than a Gyr after the interaction, the satellite galaxy usually shows a low star formation rate and, thus, an old stellar population (Wetzel et al. 2013). However, S2 looks very bright in the GALEX UV images (see Fig. 3), and thus it is actively forming stars. This result also disfavours the hypothesis that it interacted with NGC 922 to produce the observed tidal ring. In addition, the low surface brightness features detected in our image suggest that this dwarf galaxy holds its own tidal structure. Figure 4 shows an image cutout from the DESI LS data centred in this galaxy, showing the presence of a strong shell around S2. This shell-like feature looks very similar to those reported in deep images of the outskirts of the Large Magellanic Cloud (Besla et al. 2016), which possibly originated from its interaction with the Small Magellanic Cloud. This S2 tidal feature gives additional support to the hypothesis that this satellite cannot be the intruder that generated the TRG, since a low-mass system such as S2 should not hold such an unbound stellar structure after interacting with another galactic system. The detection of this structure could also be a direct proof that dwarf satellites suffer similar accretion events to their larger counterparts. Although more data are needed, this may also be a sign that S2 is just in its first infall towards NGC 922.

3.2. Stream surface brightness and colours

The photometry measurements for the stream were carried out in circular apertures placed on clearly detected parts of the stream. Regions where the stream surface brightness could be contaminated by the outer disk of NGC 922 were avoided. Figure 2 illustrates the photometry measurement approach used in our analysis. After subtracting the sky from the input images[3], the first step was to perform the detection of the signal. Then all foreground and background objects, identified as 'clumps' in Gnuastro's SEGMENT programme (Akhlaghi & Ichikawa 2015; Akhlaghi 2019), were masked and apertures were placed on the resulting image to measure the photometry parameters (e.g., surface brightness and colours). The 'shell' on the north-east side of the disk of NGC 922 (labelled as S in Fig. 1) and the 'tail' on the south-west side (labelled as T in Fig. 1) were measured separately. For comparison, the photometry parameters were also measured in an aperture placed on the galaxy.

The results for the average surface brightness and colours along with the corresponding errors are given in Table 1, computed by Gnuastro's MAKECATALOG[4]. The measurements were averaged separately for the shell and the tail described above. The surface brightness of the tail is approximately 2 mag arcsec^{-2} fainter than in the shell. The average colours differ somewhat between the shell and the tail, but are close enough (the shell colours are at 0.75σ for $(g-z)$ and 1.6σ for $(g-r)$ within the tail colour error distribution) to reinforce the notion that both parts belong to the same stream. The results are given for the DESI LS custom image, as the host galaxy-subtracted image suffers from over-subtraction and yields surface brightnesses up to 0.1 mag arcsec^{-2} fainter than for the image without subtraction for the tail, and up to 0.2 mag arcsec^{-2} fainter for the shell, as expected, while the relative comparison between the shell and the tail remains the same. Further to quantifying the effect of masking the host's disk on the photometry measurements, the robustness of the photometry values presented in Table 1 was tested in different ways: using apertures of

[3] Gnuastro applies tesselation to the image for the detection step, so that the sky estimation and subtraction is done on a local tile basis (40×40 pixels tiles were used for the 2290×2290 pixels NGC 922 image).

[4] https://www.gnu.org/software//gnuastro/manual/html_node/MakeCatalog.html

Table 1. Surface brightnesses, colours, and apparent magnitude for the tidal features detected around NGC 922.

	$\langle\mu_g\rangle$ [mag arcsec^{-2}]	$\langle\mu_r\rangle$ [mag arcsec^{-2}]	$\langle\mu_z\rangle$ [mag arcsec^{-2}]	$\langle g-r\rangle_{\rm stream}$ [mag]	$\langle g-z\rangle_{\rm stream}$ [mag]	m_g [mag]	m_r [mag]	m_z [mag]
Shell	25.85 ± 0.02	25.34 ± 0.01	24.96 ± 0.03	0.53 ± 0.01	0.87 ± 0.005	16.80 ± 0.004	16.27 ± 0.004	15.93 ± 0.003
Tail	27.92 ± 0.08	27.27 ± 0.07	27.04 ± 0.16	0.61 ± 0.05	0.84 ± 0.04	19.95 ± 0.04	19.35 ± 0.03	19.11 ± 0.03
NGC 922	22.59 ± 0.003	22.23 ± 0.003	22.21 ± 0.004	0.36 ± 0.003	0.58 ± 0.004			

Notes. For the shell (S) and for the tail (T), the measurements listed are the average of the measurements on the circular apertures placed along the stream showed in Fig. 2. We also include surface brightness and colour for NGC 922, measured using a single aperture in its nominal centre.

different shape and area, and varying configuration parameters of the detection and segmentation functions of Gnuastro. The differences in surface brightness values obtained through these changes are well below 1%, and thus we consider the level of robustness of the photometry measurements to be satisfactory.

3.3. Luminosity and stellar mass

Unfortunately, it is not possible to derive the total luminosity of NGC 922 stream, mainly because some parts of the stream are hidden by (or overlapping) the host disk, or they are too faint to be detected due to the surface brightness limit of our images. However, it is worth attempting to approximate it in order to be able to properly constrain the stellar mass of its progenitor and to better understand the impact of its interaction with NGC 922. For this purpose, the apparent magnitude and total luminosity of the stream was measured using larger apertures covering as much area as possible of their different detected pieces. Two separate polygonal apertures were placed overlapping the shell and the tail, respectively, as depicted in Fig. 2. The measured apparent magnitudes are given in Table 1.

From the apparent magnitudes given in Table 1, NGC 922 distance (d = 43.1 Mpc from Meurer et al. 2006) and the Galactic extinction obtained from NASA/IPAC Extragalactic Database[5]), we derived an absolute magnitude of $M_g = -16.5 \pm 0.04$ mag, $M_r = -17.0 \pm 0.03$ mag, and $M_z = -17.3 \pm 0.03$ mag for the whole stream (shell plus tail). We computed the luminosity of these two parts of the stream by using the solar absolute magnitudes for the g, the r, and the z passbands from Willmer (2018). We obtained the values of $4.14\times10^8\ L_\odot$ for the g passband, $4.42\times10^8\ L_\odot$ for the r passband, and $5.35\times10^8\ L_\odot$ for the z passband. We calculated the mass-to-light ratio (M/L_λ) from the three colours measured for the stream (see Sect. 3.2), using the correlations between SDSS ugriz colours and SDSS/2MASS M/L ratios given in Bell et al. (2003; i.e., the coefficients given in Table A7 of their paper). Following this method, we obtained an estimate for the stellar mass of the stream progenitor between $6.87\times10^8\ M_\odot$ and $8.51\times10^8\ M_\odot$. The ratio between the stellar masses of the dwarf progenitor and the host spiral galaxy is key to determine the kind of tidal interaction between them, and to characterize the resulting merger event. Considering the stellar mass of NGC 922 is $5.47\times10^8\ M_\odot$ (Wong et al. 2006), this yields a (stellar) mass merger ratio between 0.13 and 0.16.

4. *N*-body simulations

We performed a set of N-body simulations using the ART code (Kravtsov et al. 1997; Colín et al. 2010), starting with initial conditions designed to reproduce NGC 922-intruder interaction that generated the observed stellar plume (Pellerin et al. 2010). We used a single dark matter particle species with a mass of $2.5\times10^4\ M_\odot$, which is the same we set as the maximum star particle mass. The spatial resolution (one AMR cell side) was 40 pc.

The simulated system included an NGC 922-like and a compact dwarf galaxy, both inside a box of $1\,{\rm Mpc}\,h^{-1}$ side. The NGC 922-like galaxy was simulated as a stellar exponential disk embedded in a Navarro–Frenk–White (NFW) dark matter halo. In Table 2 we show the parameters we used to generate the stellar disk and the dark matter halo profiles. The initial conditions of the collisionless components were obtained using the Jeans equation moments method, as introduced by Hernquist (1993). We chose these parameters to be consistent with the results from our own observations of the NGC 922 system, as well as the ones by Wong et al. (2006), Pellerin et al. (2010), Elagali et al. (2018b). In contrast with previous works, we simulated the compact dwarf system as an extended distribution of particles, which allowed us to reproduce the observed stellar stream. The initial condition of this system is a simple stellar structure that follows a compact NFW profile (see Table 2).

We located the compact dwarf at (1.0,0.0,100.0) kpc, the NGC 922-like system being at (0.0,0.0,0.0) kpc, and with a relative velocity of $(0.0,0.0,-500)\,{\rm km\,s^{-1}}$. The initial location and velocity of the intruder were chosen to produce an off-centre collision, following the works by Wong et al. (2006) and Renaud et al. (2018). We evolved the system for 2 Gyr, which allowed us to study the intruder's orbit from its first infall to an almost complete disruption (see Fig. 5).

5. Discussion

In this section we analyse two scenarios for the formation of NGC 922's tidal ring structure. First, we study the currently accepted scenario where the S2 dwarf galaxy is the intruder. Then, we propose a new scenario where the intruder is a much closer satellite that is now almost completely disrupted, which also generated the umbrella-like stellar stream and the detected HI tail.

In the scenario proposed by Wong et al. (2006), S2 strongly interacted with NGC 922 and quickly moved to its current location. If we assume that NGC 922 and S2 are roughly at the same distance from the Sun (i.e., 43.1 Mpc according to Meurer et al. 2006), this means that S2 moved at a minimum distance of ~100 Kpc from NGC 922's centre. If S2 is not gravitationally bound to the central galaxy (parabolic orbit), the time interval between two positions d_1 and d_2 of the trajectory is roughly $\Delta t \sim (d_2^{3/2} - d_1^{3/2})/\sqrt{4.5GM}$. Therefore, assuming a close encounter between NGC 922 and S2, and no mass-loss, dynamical friction, or other slow-down processes, the S2 dwarf would need, at least, 0.7 Gyr to reach 100 Kpc distance from NGC 922's centre. If S2 is gravitationally bound, this time interval would be even larger. All models and simulations show that the star-forming rings associated with the tidal ring structures

[5] https://ned.ipac.caltech.edu/extinction_calculator

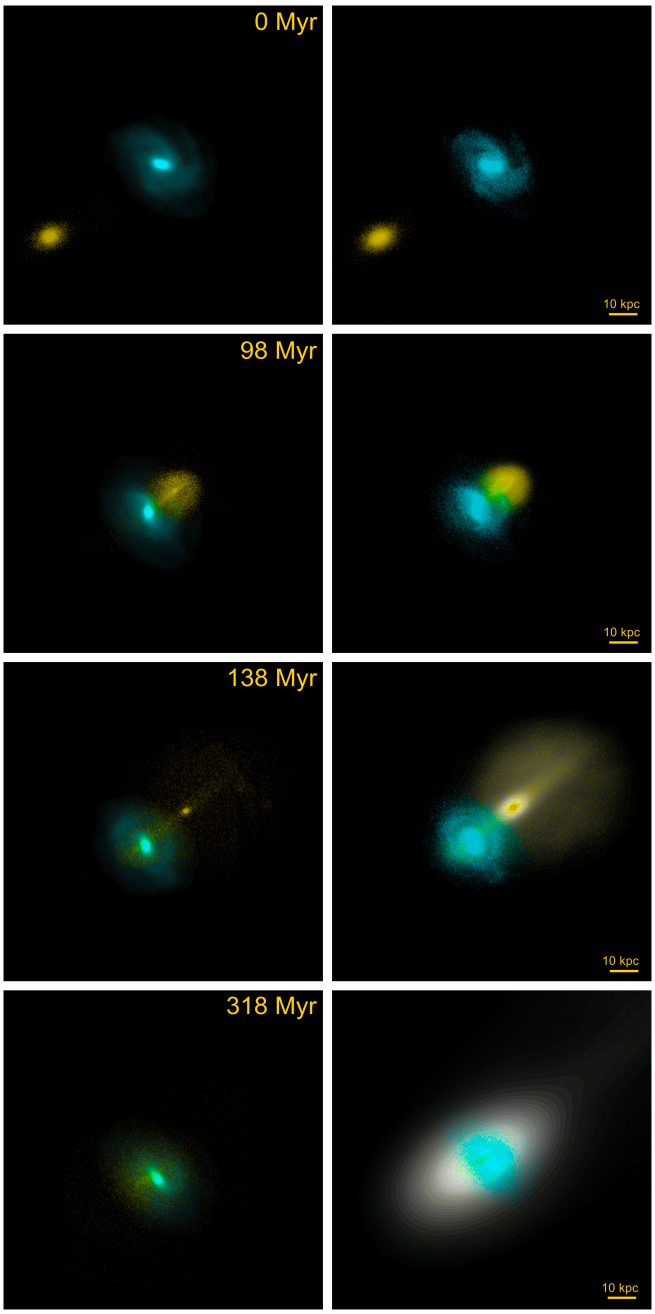

Fig. 5. Four snapshots of the *N*-body simulation of an NGC 922-like TRG formation. *Left panels*: focusing on the tidal ring formation within the main galactic system (cyan). *Right panel*: putting the focus on the intruder evolution (yellow) and on the formation of tidal shells. The zero points of the time progression labelled in the left panels are arbitrary and do not correspond to the initial conditions of the simulation.

only lasted for 0.2–0.5 Gyr (Wong et al. 2006; Pellerin et al. 2010; Renaud et al. 2018; Elagali et al. 2018a) and became only marginally observable up to 0.7 Gyr after the collision (Wu & Jiang 2015). NGC 922's star forming ring is clearly visible (see Fig. 1), so it is in an early stage of its evolution. Both results are not compatible, and therefore we state that this first scenario should be put in doubt. In addition, as discussed in Sect. 3.1, the S2 dwarf holds its own well-defined tidal shell structure, a feature that should not exist if the dwarf had a strong close encounter with NGC 922. We also warn the reader that although Wong et al. (2006) reproduced such a scenario using pure *N*-body simulations, in their models they simulated the intruder as a point mass, and thus they did not capture most of the tidal effects that affect its evolution. In this simplified model, the effects over the central galaxy structure are also artificially magnified. In our models, the intruder has internal structure and it still induces a tidal ring on the central galaxy. The largest difference between our model and the model of Wong et al. (2006) is the fate of the intruder. In agreement with previous models (see e.g., Foster et al. 2014), the intruder is partially or totally disrupted and generates a variety of tidal structures around the central galaxy (see Fig. 5). We also notice that the TRG morphology obtained in our simulations lasts for less than 500 Myr after the intruder's first pericentre, as predicted by previous works. This result reinforces the hypothesis that a recent interaction is responsible for the tidal ring structure. Finally, it is also important to mention that in most of the studied TRGs, authors detected HI tails in the direction of the intruder (see e.g., Higdon 1996). In Elagali et al. (2018b), the authors found an HI tail but it points in the other direction, extending towards the north of the disk instead of the east, and for ∼0.7 arcmin (8 Kpc). This result is also inconsistent with the simple collisional scenario proposed by Wong et al. (2006) for NGC 922's formation.

The discovery of the new stream morphology (see Sect. 3.1) and the results from our *N*-body models (see Fig. 5) brought us to a new interpretation for the origin of NGC 922 morphology. From an observational point of view, we detected that a satellite merged recently with the host, producing two shells: one evident in the north-west, another one more diffuse in the south-east, with a total mass of ∼6.9–8.5×10^8 $M_\odot$ (see also the 138 Myr snapshot in Fig. 5). After the first pericentre, the less gravitationally bounded stars of the intruder are stripped out and are trapped by the central galaxy potential well (e.g., Hendel & Johnston 2015), so we expect that stars of this dwarf satellite are now partially mixed with stars of the central galaxy (see bottom panels of Fig. 5). If the mixing truly occurred this would be reflected by a bi-modal distribution in metallicity. In Kouroumpatzakis et al. (2021) the authors found evidence of two metallicity populations in NGC 922, a result that is consistent with the new scenario presented here. Additionally, as NGC 922 is a relatively low-mass galaxy, the infalling satellites do not suffer strong ram-pressure stripping and bring fresh HI gas that fuels star formation in the main system. The recent infall of a gas-rich satellite also explains why NGC 922 has a $M_{\rm HI}/M_*$ ∼ 0.32, which is much higher than the ratio observed (∼0.13) in galaxies with similar masses (see Elagali et al. 2018b). The presence of these tidal shells can also explain the gas warps detected on the western side of NGC 922's disk, which are also evident in its velocity field (Elagali et al. 2018b) and which led some authors to propose that the system was already perturbed before the formation of the tidal ring (e.g., Renaud et al. 2018). Our *N*-body models also support this scenario, which contradicts the formerly accepted one where S2 was the intruder (see Fig. 5).

6. Conclusions

We present a new merger history for the formation of the TRG NGC 922 after obtaining a set of deep images that reveal its low surface brightness outskirts. The main conclusions of this work are the following:

- We report the presence of an umbrella-like tidal structure where previous observations proposed the presence of a connecting tidal tail with a nearby dwarf galaxy.
- The absence of such a tidal tail connecting NGC 922 with the dwarf companion S2 (PGC 3080368), both in stars or in

Table 2. Initial setup of the NGC 922-like and compact dwarf galactic systems.

Properties	NGC 922-like	Compact dwarf	
$M_{\rm tot}$ [$M_\odot$]	1.22×10^{11}	5×10^{9}	Total mass
M_* [$M_\odot$]	2.5×10^{10}	8×10^{8}	Stellar mass
$R_{\rm d}$ [kpc]	3.14		Stellar disk exponential scale length
$z_{\rm d}$ [kpc]	0.20		Stellar disk scale height
$R_{\rm dtrunc}$ [kpc]	14.30		Stellar disk truncation radius
Q	1.2		Toomre parameter
$C_{\rm NFW}$	15	10	Concentration parameter
$R_{\rm s}$ [kpc]	8.27	2.4	Halo scale radius
$R_{\rm htrunc}$ [$R_{\rm s}$]	25.0	2	Halo truncation radius in $R_{\rm s}$ units

HI, may discard the hypothesis of S2 being the trigger of the tidal ring formation. Recent works have also raised the question of whether a scenario as simple as a single off-shot could explain the many peculiar properties of this system.

– We propose a new scenario for the formation of the tidal ring in NGC 922: a merger with an already totally or partially stripped dwarf galaxy. This new scenario explains many of the previous peculiar results such as high velocities in the outskirts of the galaxy, the presence of two metallicity populations, and the relatively recent formation of the ring, if the expansion velocities and lifetimes predicted by numerical models are correct. Also, a recent gas-rich wet merger can explain the observed high HI mass fraction of the galactic system.
– Finally, we present the discovery of a tidal structure around the dwarf galaxy S2, which holds its own tidal shell structure. This, together with its high star formation rate shown by the GALEX-UV data (Fig. 3), could be evidence that the system is in its first infall towards NGC 922. This result can be confirmed by future estimations of the radial velocity and proper motions of this satellite.

Our work also showed that deep imaging of the TRG's properties, reaching a regime with enough surface brightness to detect the presence of giant tidal shells in their outskirts, can provide valuable information on the recent evolution of galaxies undergoing a minor merger. In the Stellar Tidal Stream Survey (Martínez-Delgado et al., in prep.), we have detected several nearby spiral galaxies with both tidal rings and tidal shell features in different evolutionary stages. Our observations include galaxies with recently formed tidal rings and single tenuous shells, others with well-developed tidal rings and a single shell, and also some with evidence of multiple tidal rings and shells. However, to make a systematic study of the relation between the formation of tidal rings and the almost radial minor mergers that generate tidal shells, it is fundamental to carry out a systematic survey of TRGs with a surface brightness limit fainter than 28 mag arcsec^{-2}. Once completed, this deep imaging survey combined with future space missions such as EUCLID will provide us with enough data to fully characterize the TRG in the local volume and, thus, to better understand the processes that shape galaxies during and after a radial minor merger. This information will also open the door to study whether the Milky Way suffered such a process in its recent history.

Acknowledgements. DMD acknowledges financial support from the Talentia Senior Program (through the incentive ASE-136) from Secretaría General de Universidades, Investigación y Tecnología, de la Junta de Andalucía. DMD acknowledges funding from the State Agency for Research of the Spanish MCIU through the "Center of Excellence Severo Ochoa" award to the Instituto de Astrofísica de Andalucía (SEV-2017-0709) and project (PDI2020-114581GB-C21/ AEI / 10.13039/501100011033). SRF acknowledges financial support from the Spanish Ministry of Economy and Competitiveness (MINECO) under grant number AYA2016-75808-R, AYA2017-90589-REDT and S2018/NMT-429, and from the CAM-UCM under grant number PR65/19-22462. SRF acknowledges support from a Spanish postdoctoral fellowship, under grant number 2017-T2/TIC-5592. MAGF acknowledges financial support from the Spanish Ministry of Science and Innovation through the project PID2020-114581GB-C22. JR acknowledges support from the State Research Agency (AEI-MCINN) of the Spanish Ministry of Science and Innovation under the grant "The structure and evolution of galaxies and their central regions" with reference PID2019-105602GB-I00/10.13039/501100011033. JR also acknowledges funding from University of La Laguna through the Margarita Salas Program from the Spanish Ministry of Universities ref. UNI/551/2021-May 26, and under the EU Next Generation. MA acknowledges the financial support from the Spanish Ministry of Science and Innovation and the European Union – NextGenerationEU through the Recovery and Resilience Facility project ICTS-MRR-2021-03-CEFCA. This project uses data from observations at Cerro Tololo Inter-American Observatory, National Optical Astronomy Observatory, which is operated by the Association of Universities for Research in Astronomy (AURA) under a cooperative agreement with the National Science Foundation. We acknowledge support from the Spanish Ministry for Science, Innovation and Universities and FEDER funds through grant AYA2016-81065-C2-2. We also used data obtained with the Dark Energy Camera (DECam), which was constructed by the Dark Energy Survey (DES) collaboration. Funding for the DES Projects has been provided by the US Department of Energy, the US National Science Foundation, the Ministry of Science and Education of Spain, the Science and Technology Facilities Council of the United Kingdom, the Higher Education Funding Council for England, the National Center for Supercomputing Applications at the University of Illinois at Urbana-Champaign, the Kavli Institute of Cosmological Physics at the University of Chicago, the Center for Cosmology and Astro-Particle Physics at the Ohio State University, the Mitchell Institute for Fundamental Physics and Astronomy at Texas A&M University, Financiadora de Estudos e Projetos, Fundação Carlos Chagas Filho de Amparo à Pesquisa do Estado do Rio de Janeiro, Conselho Nacional de Desenvolvimento Científico e Tecnológico and the Ministério da Ciência, Tecnologia e Inovacão, the Deutsche Forschungsgemeinschaft, and the Collaborating Institutions in the Dark Energy Survey. The Collaborating Institutions are Argonne National Laboratory, the University of California at Santa Cruz, the University of Cambridge, Centro de Investigaciones Enérgeticas, Medioambientales y Tecnológicas-Madrid, the University of Chicago, University College London, the DES-Brazil Consortium, the University of Edinburgh, the Eidgenössische Technische Hochschule (ETH) Zürich, Fermi National Accelerator Laboratory, the University of Illinois at Urbana-Champaign, the Institut de Ciències de l'Espai (IEEC/CSIC), the Institut de Física d'Altes Energies, Lawrence Berkeley National Laboratory, the Ludwig-Maximilians Universität München and the associated Excellence Cluster Universe, the University of Michigan, the National Optical Astronomy Observatory, the University of Nottingham, the Ohio State University, the University of Pennsylvania, the University of Portsmouth, SLAC National Accelerator Laboratory, Stanford University, the University of Sussex, and Texas A&M University. Support for this work was provided by NASA through the NASA Hubble Fellowship grant #HST-HF2-51466.001-A awarded by the Space Telescope Science Institute, which is operated by the Association of Universities for Research in Astronomy, Incorporated, under NASA contract NAS5-26555. This work was partly done using GNU Astronomy Utilities (Gnuastro, ascl.net/1801.009) version 0.17. Work on Gnuastro has been funded by the Japanese MEXT scholarship and its Grant-in-Aid for Scientific Research (21244012, 24253003), the European Research Council (ERC) advanced grant 339659-MUSICOS, and from the Spanish Ministry of Economy and Competitiveness (MINECO) under grant

number AYA2016-76219-P. M.A acknowledges the financial support from the Spanish Ministry of Science and Innovation and the European Union – NextGenerationEU through the Recovery and Resilience Facility project ICTS-MRR-2021-03-CEFCA.

References

Abbott, T. M. C., Abdalla, F. B., Allam, S., et al. 2018, ApJS, 239, 18
Akhlaghi, M. 2019, Proceedings of the International Astronomical Union (S355), 2020
Akhlaghi, M., & Ichikawa, T. 2015, ApJS, 220, 1
Barway, S., Mayya, Y. D., & Robleto-Orús, A. 2020, MNRAS, 497, 44
Bell, E. F., McIntosh, D. H., Katz, N., & Weinberg, M. D. 2003, ApJS, 149, 289
Besla, G., Martínez-Delgado, D., van der Marel, R. P., et al. 2016, ApJ, 825, 20
Buta, R. 1995, ApJS, 96, 39
Buta, R. J. 2017, MNRAS, 471, 4027
Buta, R., & Combes, F. 1996, Fund. Cosmic Phys., 17, 95
Charmandaris, V., Laurent, O., Mirabel, I. F., et al. 1999, A&A, 341, 69
Colín, P., Avila-Reese, V., Vázquez-Semadeni, E., Valenzuela, O., & Ceverino, D. 2010, ApJ, 713, 535
Dey, A., Schlegel, D. J., Lang, D., et al. 2019, AJ, 157, 168
Elagali, A., Lagos, C. D. P., Wong, O. I., et al. 2018a, MNRAS, 481, 2951
Elagali, A., Wong, O. I., Oh, S.-H., et al. 2018b, MNRAS, 476, 5681
Elmegreen, D. M., & Elmegreen, B. G. 2006, ApJ, 651, 676
Erwin, P. 2015, ApJ, 799, 226
Fiacconi, D., Mapelli, M., Ripamonti, E., & Colpi, M. 2012, MNRAS, 425, 2255
Fogarty, L., Thatte, N., Tecza, M., et al. 2011, MNRAS, 417, 835
Foster, C., Lux, H., Romanowsky, A. J., et al. 2014, MNRAS, 442, 3544
Gerber, R. A., Lamb, S. A., & Balsara, D. S. 1992, ApJ, 399, L51
Gerber, R. A., Lamb, S. A., & Balsara, D. S. 1996, MNRAS, 278, 345
Hendel, D., & Johnston, K. V. 2015, MNRAS, 454, 2472
Hernquist, L. 1993, ApJS, 86, 389
Hernquist, L., & Weil, M. L. 1993, MNRAS, 261, 804
Higdon, J. L. 1996, ApJ, 467, 241
Kormendy, J., & Kennicutt, R. C., Jr 2004, ARA&A, 42, 603
Kouroumpatzakis, K., Zezas, A., Wolter, A., et al. 2021, MNRAS, 500, 962
Kravtsov, A. V., Klypin, A. A., & Khokhlov, A. M. 1997, ApJS, 111, 73
L'Huillier, B., Combes, F., & Semelin, B. 2012, A&A, 544, A68
Lynds, R., & Toomre, A. 1976, ApJ, 209, 382
Madore, B. F., Nelson, E., & Petrillo, K. 2009, ApJS, 181, 572
Martínez-Delgado, D., Gabany, R. J., Crawford, K., et al. 2010, AJ, 140, 962
Martinez-Delgado, D., Cooper, A.P., Roman, J., et al. 2021, arXiv e-prints [arXiv:2104.06071]
Mayya, Y. D., Bizyaev, D., Romano, R., Garcia-Barreto, J. A., & Vorobyov, E. I. 2005, ApJ, 620, L35
Meurer, G. R., Hanish, D. J., Ferguson, H. C., et al. 2006, ApJS, 165, 307
Nair, P. B., & Abraham, R. G. 2010, ApJS, 186, 427
Pellerin, A., Meurer, G. R., Bekki, K., et al. 2010, AJ, 139, 1369
Renaud, F., Athanassoula, E., Amram, P., et al. 2018, MNRAS, 473, 585
Román, J., Trujillo, I., & Montes, M. 2020, A&A, 644, A42
Romero-Gómez, M., Athanassoula, E., Masdemont, J. J., & García-Gómez, C. 2007, A&A, 472, 63
Struck-Marcell, C. 1990, AJ, 99, 71
Theys, J. C., & Spiegel, E. A. 1976, ApJ, 208, 650
Wetzel, A. R., Tinker, J. L., Conroy, C., & van den Bosch, F. C. 2013, MNRAS, 432, 336
Willett, K. W., Lintott, C. J., Bamford, S. P., et al. 2013, MNRAS, 435, 2835
Willmer, C. N. A. 2018, ApJS, 236, 47
Wong, O. I., Meurer, G. R., Bekki, K., et al. 2006, MNRAS, 370, 1607
Wu, Y.-T., & Jiang, I.-G. 2012, ApJ, 745, 105
Wu, Y.-T., & Jiang, I.-G. 2015, ApJ, 805, 32
Zou, H., Zhou, X., Fan, X., et al. 2019, ApJS, 245, 4